

# Artemisinins target the SERCA of *Plasmodium falciparum*

U. Eckstein-Ludwig<sup>1</sup>, R. J. Webb<sup>1</sup>, I. D. A. van Goethem<sup>2</sup>, J. M. East<sup>2</sup>, A. G. Lee<sup>2</sup>, M. Kimura<sup>3</sup>, P. M. O'Neill<sup>4</sup>, P. G. Bray<sup>5</sup>, S. A. Ward<sup>5</sup> & S. Krishna<sup>1</sup>

<sup>1</sup>Department of Cellular and Molecular Medicine, St George's Hospital Medical School, Cranmer Terrace, London SW17 0RE, UK

<sup>2</sup>Department of Biochemistry and Molecular Biology, University of Southampton, Southampton SO16 7PX, UK

<sup>3</sup>Radioisotope Centre, Osaka City University Medical School, Asahi-machi 1-4-3, Abeno-ku, Osaka 545-8585, Japan

<sup>4</sup>Department of Chemistry, The Robert Robinson Laboratories, University of Liverpool, Liverpool L69 7ZD, UK

<sup>5</sup>Molecular and Biochemical Parasitology Group, Liverpool School of Tropical Medicine, Pembroke Place, Liverpool L3 5QA, UK

Artemisinins are extracted from sweet wormwood (*Artemisia annua*) and are the most potent antimalarials available<sup>1</sup>, rapidly killing all asexual stages of *Plasmodium falciparum*<sup>2</sup>. Artemisinins are sesquiterpene lactones widely used to treat multidrug-resistant malaria<sup>1</sup>, a disease that annually claims 1 million lives. Despite extensive clinical and laboratory experience<sup>3–5</sup> their molecular target is not yet identified. Activated artemisinins form adducts with a variety of biological macromolecules, including haem, translationally controlled tumour protein (TCTP) and other higher-molecular-weight proteins<sup>6</sup>. Here we show that artemisinins, but not quinine or chloroquine, inhibit the SERCA orthologue (PfATP6) of *Plasmodium falciparum* in *Xenopus* oocytes with similar potency to thapsigargin (another sesquiterpene lactone and highly specific SERCA inhibitor). As predicted, thapsigargin also antagonizes the parasitocidal activity of artemisinin. Desoxyartemisinin lacks an endoperoxide bridge and is ineffective both as an inhibitor of PfATP6 and as an antimalarial. Chelation of iron by desferrioxamine abrogates the antiparasitic activity of artemisinins and correspondingly attenuates inhibition of PfATP6. Imaging of parasites with BODIPY-thapsigargin labels the cytosolic compartment and is competed by artemisinin. Fluorescent artemisinin labels parasites similarly and irreversibly in an Fe<sup>2+</sup>-dependent manner. These data provide compelling evidence that artemisinins act by inhibiting PfATP6 outside the food vacuole after activation by iron.

Some<sup>3,7</sup>, but not all<sup>8–10</sup>, studies suggest that artemisinins act by haem-dependent activation of an endoperoxide bridge occurring within the parasite's food vacuole. However, localization of artemisinins to parasite and not food vacuole membranes<sup>11</sup>, and killing of tiny rings lacking haemozoin argue against the food vacuole being a major site for drug action<sup>2</sup>. Artemisinins show structural similarities to thapsigargin, which is a highly specific inhibitor of sarco/endoplasmic reticulum Ca<sup>2+</sup>-ATPase (SERCA). We therefore hypothesized that when activated, artemisinins act by specifically and selectively inhibiting the SERCA of *P. falciparum*.

PfATP6 is the only SERCA-type Ca<sup>2+</sup>-ATPase sequence in the parasite's genome. We expressed PfATP6 in *Xenopus laevis* oocytes because it could not be functionally assayed in COS cells (J.M.E., unpublished work). Membrane preparations from oocytes expressing PfATP6 consistently gave higher Ca<sup>2+</sup>-dependent ATPase activities than water-injected control oocytes (mean ± s.e.m. activities of 0.054 ± 0.006 IU compared with 0.026 ± 0.003 international units (IU), *n* = 25; *P* < 0.0001). These activities are comparable to those observed with PfATP4, another *P. falciparum* Ca<sup>2+</sup>-ATPase<sup>12</sup>. Figure 1a compares the Ca<sup>2+</sup>-activation profiles of PfATP6 and rabbit skeletal muscle SERCA1a (sarcolemmal preparation) and shows that PfATP6 and SERCA1a are acti-

vated by similar concentrations of Ca<sup>2+</sup> ions, [Ca<sup>2+</sup>]<sub>free</sub> (Fig. 1a and ref. 12). PfATP6 (like SERCA1a) is inhibited by thapsigargin and cyclopiazonic acid, but not by ouabain, a specific Na<sup>+</sup>/K<sup>+</sup>-ATPase inhibitor (Fig. 1b). Vanadate, which is a more general inhibitor of P-type ATPases, also inhibits PfATP6.

We then assessed the inhibitory properties of chloroquine (a 4-aminoquinoline), quinine (a cinchona alkaloid) and artemisinin on transporter proteins encoded by *P. falciparum* and expressed in *Xenopus* oocytes, as well as their effects on SERCA1a. Supratherapeutic concentrations of these antimalarials did not inhibit glucose transport by the falciparum hexose transporter (PfHT), confirming that none of these structurally diverse compounds

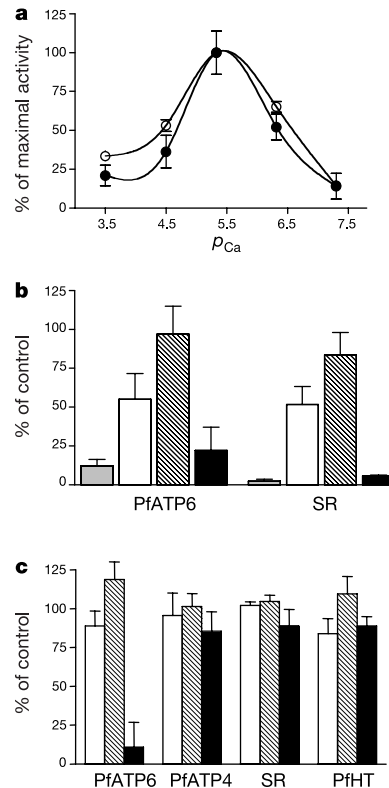


**Figure 1** Functional characterization of PfATP6. **a**, Ca<sup>2+</sup>-dependency of PfATP6 activity (filled circles) compared with SERCA1a (SR) activity (open circles) is shown as a percentage of maximal activity (normalized to the maximum value, and not corrected for endogenous activity for PfATP6) at the indicated [Ca<sup>2+</sup>]<sub>free</sub> values. *p*<sub>Ca</sub> = -log<sub>10</sub>[Ca<sup>2+</sup>]<sub>free</sub>. Bars with each symbol represent standard errors for each assay (a minimum of three experiments for sarcoplasmic reticulum (SR) and seven for PfATP6). Half-maximal activation is achieved at [Ca<sup>2+</sup>]<sub>free</sub> values of 0.64 μM for PfATP6 and 0.3 μM for SERCA. Maximal activation is at [Ca<sup>2+</sup>]<sub>free</sub> of 48 μM for both PfATP6 and SERCA. **b**, Inhibitor profiles for PfATP6 and SERCA. ATPase activities were determined with inhibitors and are compared with control values: thapsigargin (grey bar, 0.8 μM, *P* < 0.0001; multivariate analysis of variance, MANOVA), sodium orthovanadate (white bar, 100 μM, *P* = 0.043), ouabain (hatched bar, 100 μM, *P* = 0.87), and cyclopiazonic acid (black bar, 1 μM, *P* = 0.0033). Each bar represents a minimum of six experiments. **c**, Effects of antimalarials on two *P. falciparum* Ca<sup>2+</sup>-ATPases (PfATP6 and PfATP4), the *P. falciparum* hexose transporter (PfHT) and mammalian SERCA (SR). All activities are shown as a percentage of uninhibited activity and are compared with these activities: quinine (open bars, 10 μM, *P* > 0.1; MANOVA), chloroquine (hatched bar, 1 μM, *P* > 0.1), artemisinin (black bars; 50 μM, *P* > 0.1 for PfATP4, SR, PfHT; 1 μM for PfATP6, *P* < 0.0001). Ca<sup>2+</sup>-ATPase activity for PfATP6 is shown after correction of Ca<sup>2+</sup>-ATPase activity measured in water-injected oocytes, which was unnecessary for PfATP4, because there was no inhibition observed with any antimalarial. Each bar represents a minimum of four experiments.

interferes non-specifically with the function of integral membrane proteins of *P. falciparum* (Fig. 1c). SERCA1a activity was also unaffected by these antimalarials. Apart from PfATP6, PfATP4 is the only  $\text{Ca}^{2+}$ -ATPase-like sequence identified in the *P. falciparum* genome, and defines a non-SERCA subclass of  $\text{Ca}^{2+}$ -ATPase that is

unique to apicomplexan organisms<sup>12</sup>. PfATP4 activity was also not inhibited by any of the antimalarials tested. In contrast,  $\text{Ca}^{2+}$ -dependent ATPase activity of PfATP6 was abolished by artemisinin, but not by quinine or chloroquine. These data show that even at relatively high concentrations (1  $\mu\text{M}$ ) artemisinin inhibits PfATP6

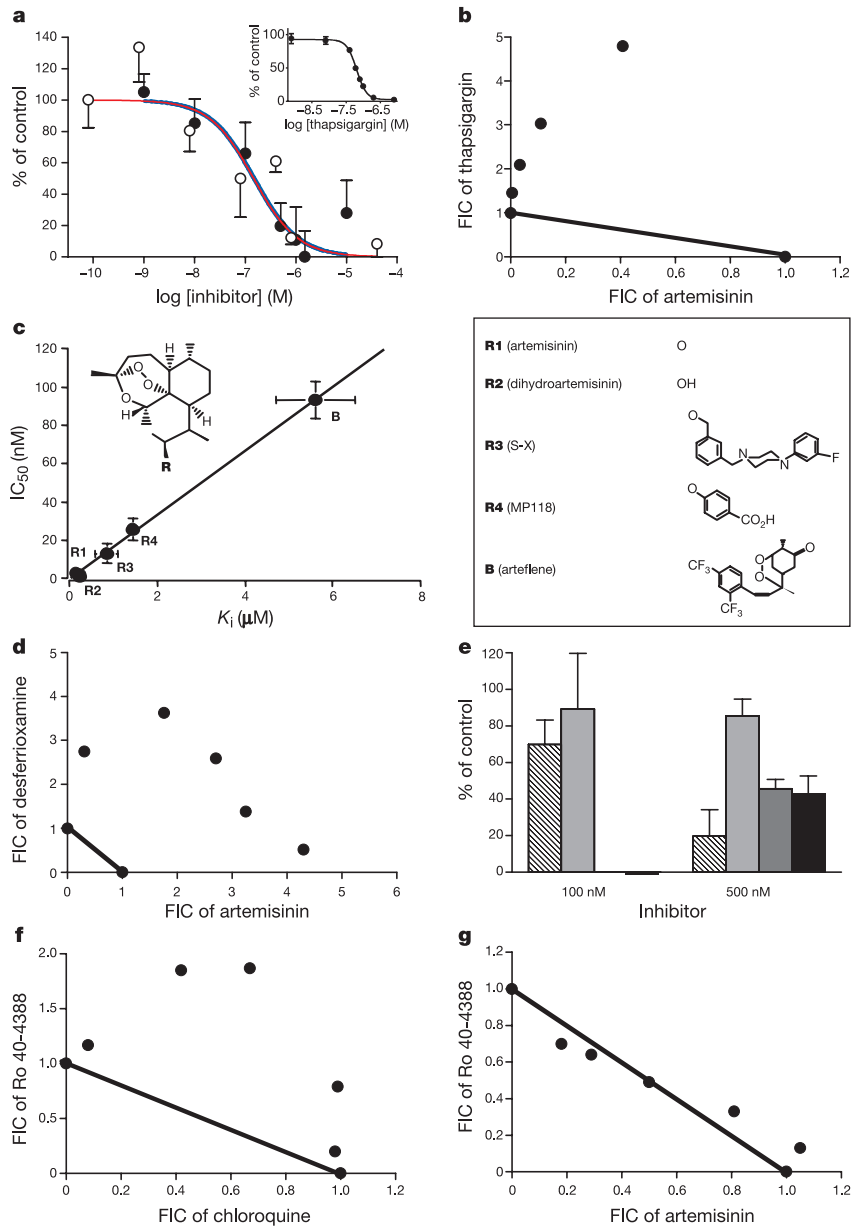


**Figure 2** Properties of artemisinin inhibition. **a**, The half-maximal inhibition constants ( $K_i$ ) for artemisinin (black circles, blue line,  $162 \pm 31$  nM) and thapsigargin (white circles, red line,  $146 \pm 66$  nM) were determined. For thapsigargin endogenous  $\text{Ca}^{2+}$ -ATPase activity was not subtracted, because  $K_i$  values for both activities are indistinguishable, and endogenous effects can be neglected. Because of the insensitivity of endogenous activity to artemisinin, this endogenous  $\text{Ca}^{2+}$ -ATPase component was determined at high artemisinin concentration (50  $\mu\text{M}$ ) in PfATP6-expressing oocytes, and used to correct values.  $K_i$  values for thapsigargin and artemisinin are not significantly different ( $P = 0.58$ ). Data are from a minimum of three experiments. The inset shows the determination of  $K_i$  for SERCA1a-rich rabbit-muscle preparation ( $K_i = 64$  nM). **b**, An isobologram for thapsigargin and artemisinin. The solid line indicates an isobole where drugs act additively and independently. Data points above this line indicate antagonism between drugs, and data below this line would indicate synergy<sup>30</sup>. FIC is fractional inhibitory concentration. **c**, The relationship between inhibition of PfATP6 activities

determined in *Xenopus* oocyte preparations is shown compared with inhibitory potencies of artemisins whose structures are also given. Data are mean values (from a minimum of three independent experiments) with standard error bars, where visible. **d**, An isobologram for desferrioxamine and artemisinin. Interpretation is as for **b**. **e**, PfATP6 activity (corrected for endogenous activity) was determined at two different artemisinin concentrations without (hatched bars) and in presence of desferrioxamine (100  $\mu\text{M}$ , light grey bars). At 500 nM there is significant ( $P = 0.0093$ ) abrogation of inhibition of PfATP6 by artemisinin. PfATP6 activity (not corrected for endogenous) was also determined at one thapsigargin concentration without (dark grey bars) and in the presence of desferrioxamine (100  $\mu\text{M}$ , black bar). There is no significant difference in inhibitory potency ( $P > 0.5$ ). Each bar represents at least six experiments. **f**, An isobologram for chloroquine and Ro 40-4388. Interpretation is as for **b**. **g**, An isobologram for artemisinin and Ro 40-4388. Interpretation is as for **b**.

with high specificity. No other transporter, including SERCA1a, is inhibited by artemisinin even when used at 50 times (50  $\mu\text{M}$ , Fig. 1c) the concentration used to inhibit PfATP6 activity in this experiment (1  $\mu\text{M}$ ). Endogenous (oocyte)  $\text{Ca}^{2+}$ -dependent ATPase activity is also resistant to the action of artemisinin (data not shown), demonstrating the unique specificity of artemisinins for PfATP6.

To compare the interactions of artemisinin and thapsigargin with PfATP6, we measured inhibitory constants for these compounds in oocytes. Thapsigargin irreversibly inhibits  $\text{Ca}^{2+}$ -dependent ATPase activity of SERCA with 1:1 stoichiometry<sup>13</sup>. Remarkably, the inhibitory profile of artemisinin is exactly superimposable over that of thapsigargin (Fig. 2a), showing that they inhibit PfATP6 with the same potency and stoichiometry *in vitro*. Artemisinin concentrations that inhibit PfATP6 activity in oocytes ( $K_i \approx 150 \text{ nM}$ ) are somewhat higher than those required to kill cultured parasites (median  $\text{IC}_{50} = 5.47 \text{ nM}$  (range  $\text{IC}_{50} = 0.47 - 27.1 \text{ nM}$ ) artesunate;  $n = 256$  (ref. 14), and Fig. 2c).

This is unsurprising for several reasons. First, there is no information on the concentrations of artemisinins at their sub-cellular sites of action, although artemisinins are clearly concentrated in infected erythrocytes by several hundred-fold<sup>15</sup>. Second, the extent of inhibition of PfATP6 required to kill parasites is not yet determined (it may, for example, be less than the  $K_i$  value determined in oocytes). Third, our *in vitro* assays are conducted over relatively short periods of time (<15 min) whereas parasite killing is determined after exposure to drug for many hours, and killing is also enhanced in a time-dependent manner<sup>2</sup>. Fourth, the oocyte membrane preparation that we use has relatively little target protein (about 1%<sup>12</sup>) in relation to the amount of lipid, favouring sequestration of lipid-soluble components away from target protein.

Figure 2a (inset) shows that the  $K_i$  for thapsigargin on SERCA1a-rich rabbit-muscle preparations (containing protein 80% of which is SERCA1a) is 64 nM, almost double the  $\text{IC}_{50}$  value for lymphocytes (35 nM).

As both artemisinin and thapsigargin specifically inhibit PfATP6 after heterologous expression, we predicted that they would exhibit mutual antagonism in cultured parasites. Artemisinin and thapsigargin were administered simultaneously in varying concentrations, and the results plotted as an isobologram (Fig. 2b). The plot shows significant antagonism of the two drugs, indicating that artemisinin specifically inhibits PfATP6 in intact parasites, just as it does in the heterologous expression system. The higher  $\text{IC}_{50}$  value for thapsigargin in parasite culture ( $\text{IC}_{50} = 2.55 \mu\text{M}$ ) compared with the inhibitory constant for PfATP6 in oocyte membranes ( $K_i = 146 \text{ nM}$ ) may reflect difficulties in accessing intraparasitic PfATP6. This is probably because multiple membranes need to be crossed in parasites, but not in mammalian cells, which are killed by nanomolar concentrations of thapsigargin (discussed below).

To confirm that PfATP6 is the target for artemisinins we compared inhibitory constants of a range of artemisinin derivatives against PfATP6 in oocytes, with their ability to kill parasites *in vitro*. Figure 2c shows results for artemisinin, dihydroartemisinin (the principal antimalarial metabolite of many artemisinin derivatives including artesunate, artemether and artemotil), two other artemisinin derivatives (MP118 and S-X) and arteflene, a less effective semi-synthetic endoperoxide derivative. There is almost perfect correlation between inhibitory potencies of artemisinins for PfATP6 activity and  $\text{IC}_{50}$  values from cultured parasites ( $r^2 = 0.999$ , Fig. 2c). Those artemisinins that are active antimalarials all contain an endoperoxide bridge<sup>16</sup>, a key structural feature

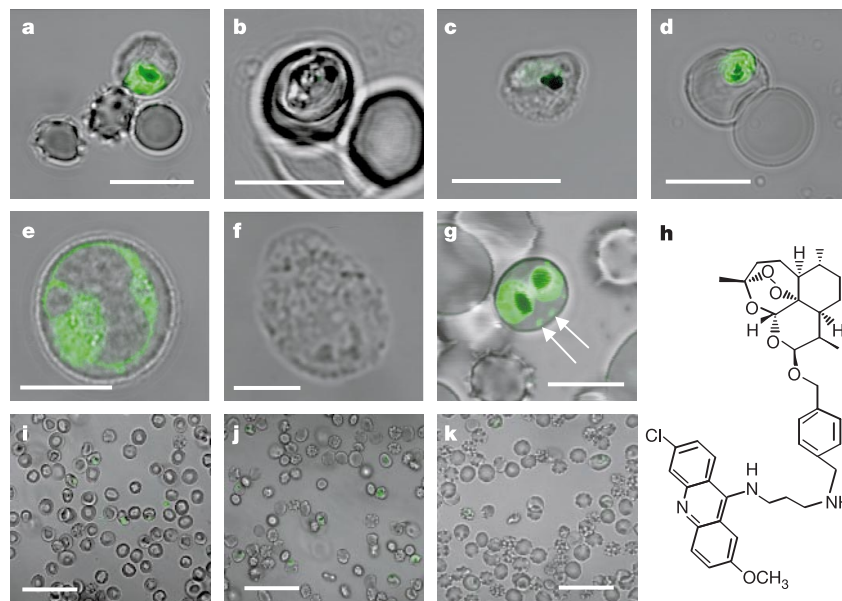


**Figure 3** *In vivo* labelling with BODIPY-thapsigargin and fluorescent-labelled artemisinin. Cells were incubated in 200 nM BODIPY-thapsigargin (10 min, 37  $^{\circ}\text{C}$ , in presence of 0.025% Pluronic F127), then washed three times and imaged. Pictures were taken after a preliminary scan, to minimize bleaching. Preincubations with unlabelled substances were performed 40 min (37  $^{\circ}\text{C}$ ) before incubation with BODIPY-thapsigargin. Artemisinin labelling (500 nM) was performed in absence of Pluronic F127. Scale bars represent 10  $\mu\text{m}$ , unless stated otherwise. **a**, Fluorescence after incubation in BODIPY-thapsigargin in a single infected cell. **b**, BODIPY-thapsigargin signal detected after preincubation in thapsigargin (50  $\mu\text{M}$ ). **c**, BODIPY-thapsigargin signal detected after preincubation in artemisinin (50  $\mu\text{M}$ ). **d**, BODIPY-thapsigargin signal detected after preincubation in artemisinin (50  $\mu\text{M}$ ) and desferrioxamine (100  $\mu\text{M}$ ). **e**, BODIPY-thapsigargin distribution

in the lymphocyte cell line PM-1, showing typical SERCA-type distribution. **f**, PM-1 cell labelled with BODIPY-thapsigargin after competition with unlabelled thapsigargin (50  $\mu\text{M}$ ). **g**, Distribution of labelled artemisinin in live parasites. Arrows indicate artemisinin in erythrocyte cytosol. **h**, Chemical structure of labelled artemisinin. **i**, Low magnification image of live parasites labelled with artemisinin (scale bar represents approximately 30  $\mu\text{m}$ ). **j**, After incubation in labelled artemisinin, cells were washed in 10-fold excess of unlabelled artemisinin and imaged (scale bar represents approximately 30  $\mu\text{m}$ ). **k**, Before incubation in labelled artemisinin, cells were pre-treated with desferrioxamine (100  $\mu\text{M}$ , 30 min), and after labelling washed as in **j** (scale bar represents approximately 30  $\mu\text{m}$ ).

that generates carbon-centred short-lived radicals through iron-mediated catalysis. These intermediate radicals react with and incapacitate target protein(s). Desoxyderivatives are otherwise structurally identical to artemisinins but lack both an endoperoxide bridge and significant antimalarial activity. We predicted that desoxyartemisinin would be a significantly less effective inhibitor of PfATP6. Desoxyartemisinin does not inhibit PfATP6 activity even at concentrations that are two orders of magnitude greater (50  $\mu\text{M}$ ) than inhibitory concentrations of artemisinin itself. Again, this observation is consistent with the  $\text{IC}_{50}$  value for desoxyartemisinin determined against parasites *in vitro* (mean  $4.85 \pm 1.7 \mu\text{M}$ ).

The generation of biologically reactive species from artemisinins depends on cleavage of the peroxide bridge via an iron-dependent mechanism. Consequently, in cultures of *P. falciparum*, iron deprivation using tight-binding chelators such as desferrioxamine may inhibit antimalarial activity<sup>17</sup>. We confirmed this antagonistic interaction between iron-deprivation and artemisinins<sup>17</sup> by isobologram analysis (Fig. 2d). If our hypothesis is correct, iron chelation should also specifically block the inhibitory effects of artemisinin in our oocyte model. Desferrioxamine abolishes the inhibitory activity of artemisinin on PfATP6 but does not alter the inhibitory properties of thapsigargin (Fig. 2e). On the basis of these observations and published data, we suggest the following model for the antimalarial action of artemisinins.

Artemisinins produce carbon-centred free radicals in the presence of catalytic quantities of  $\text{Fe}^{2+}$  with the selective targeting of PfATP6 by activated artemisinins being determined by structural features that depend on their sesquiterpene moiety. This proposed mechanism of action contrasts with suggestions that artemisinins may, like chloroquine, bind to haem and interfere with the process of haem crystallization. We therefore tested the relevance of this latter hypothesis using a protease inhibitor (Ro 40-4388)<sup>18</sup> that inhibits plasmepsin activity, blocks the first step in haemoglobin degradation and prevents the release of haem *in situ*. Chloroquine and Ro 40-4388 exhibit mutual antagonism in isobologram analysis (Fig. 2f) as expected if the mode of action of chloroquine stems from binding of the drug to haem, whereas there is neither antagonism nor synergism between Ro 40-4388 and artemisinin (Fig. 2g). This finding confirms that  $\text{Fe}^{2+}$ -dependent activation and antimalarial activity of artemisinins is independent of haem binding.

To prove a direct interaction between artemisinins and PfATP6, we used a fluorescent derivative of thapsigargin (BODIPY-thapsigargin) to localize it in parasites (Fig. 3a) and demonstrated that competition with an excess of unlabelled thapsigargin abolished this characteristic labelling of parasites (Fig. 3b; for example from 3.7% labelled parasite cells to 0%). Competition was also observed with an excess of artemisinin (Fig. 3c; reducing labelling from 3.7% to 0.84%;  $P < 0.0001$ ; in one example of three independent experiments), confirming that both artemisinin and thapsigargin interact at a similar site within the parasite. Consistent with the requirement for iron to activate artemisinin, adding desferrioxamine together with artemisinin abolished competition for thapsigargin-binding sites and restored labelling of parasites by BODIPY-thapsigargin (Fig. 3d). To confirm that interaction with PfATP6 was specific for artemisinin, we examined labelling of parasites by thapsigargin in the presence of quinine and found that this labelling was unaffected (not shown). We further confirmed the specificity of these results using BODIPY-thapsigargin to demonstrate the characteristic SERCA pattern of labelling in mammalian cells (PM-1, Fig. 3e)<sup>19</sup> and abolition of labelling after preincubation with an excess of unlabelled thapsigargin (Fig. 3f).

We next synthesized a fluorescent artemisinin derivative (Fig. 3h) and used this to image the distribution of artemisinin in infected erythrocytes (Fig. 3g). Artemisinin distributes like BODIPY-thapsigargin to membranous structures in the cytoplasm of parasites, and does not localize to the parasite food vacuole. Unlike BODIPY-thapsigargin, the fluorescent artemisinin derivative also

labels membranous structures within the cytoplasm of the host erythrocyte (Fig. 3g, arrows); these structures are identical to a tubovesicular membranous network that transports artemisinin through the host cell compartment and into the intraerythrocytic parasite<sup>20</sup>. Artemisinins are thought to interact initially with a carrier before accessing the tubovesicular membranous network, resulting in a highly efficient delivery pathway<sup>20</sup>. The fact that similar erythrocytic structures are not observed with BODIPY-thapsigargin suggests that a comparable mechanism of delivery to parasites does not exist. Poor penetration of infected erythrocytes by thapsigargin may explain why cultured parasites are relatively unsusceptible to the compound, even though inhibitory constants for thapsigargin and artemisinin against PfATP6 expressed in oocytes are similar. We further show in Fig. 3i–k that *in vivo* binding of artemisinin to parasites is not diminished by an excess of unlabelled artemisinin, unless parasites have been previously exposed to desferrioxamine, when a substantial proportion of labelled artemisinin is removable.

Artemisinin forms covalent adducts with four major membrane-associated parasite proteins (relative molecular mass,  $M_r$ , 25K, 50K, 65K and  $>200\text{K}$ ) as shown in previous studies<sup>21</sup>. Only one of these adducts has been investigated (TCTP, 25K)<sup>22</sup>, and it has not been functionally characterized, so that inhibition of other parasite proteins by artemisinins may still play an as-yet-unspecified role. A dimeric configuration for PfATP6 would predict an adduct of about 280K, consistent with the largest molecular species labelled by artemisinin. Furthermore, exposure to artemisinins rapidly causes swelling of endoplasmic reticulum in parasites, providing a morphological correlate for our proposed site of action<sup>23</sup>.

Withering<sup>24</sup> first described the therapeutic use of purple foxglove extracts containing digitalis in 1785, although mammalian  $\text{Na}^+/\text{K}^+$ -ATPases were not identified as the drug target of digitoxin, an active compound in these preparations, until 1953 (ref. 25). Our studies suggest that *Artemisia* extracts, used for an even longer period of time in China, also selectively inhibit a P-type ATPase of the malarial parasite. These results validate P-type ATPases as a drug target of human pathogens. The recent structural solution of mammalian SERCAs will aid in understanding selective toxicity of artemisinins and in producing congeners<sup>13,26</sup>. □

## Methods

### Expression studies

For functional studies in *X. laevis* oocytes the gene encoding PfATP6 was ligated into pMos blue (linearized with *EcoRV*) using a TA cloning strategy after strengthening of the Kozak consensus (accession number AJ532679). It was then sub-cloned into the *Xenopus* expression vector pcDNA3.1 (+) using flanking *BamHI* and *XbaI* restriction sites, and linearized with *XbaI*. Capped complementary RNA was transcribed (T7-mMESSAGE mMACHINE kit, Ambion, Austin, TX)<sup>27</sup>. *X. laevis* oocytes were prepared, microinjected, and total membrane preparations harvested after 4–5 days as described<sup>12,27</sup>. Sarcoplasmic reticulum (enriched for SERCA1a) was prepared from skeletal muscle of New Zealand White rabbits as described<sup>28</sup>.

### $\text{Ca}^{2+}$ -ATPase assay

$\text{Ca}^{2+}$ -ATPase activity was measured (10  $\mu\text{g}$  total protein, 25 °C) using a coupled enzyme assay as described<sup>28</sup> (CamSpec, Cambridge, UK).  $[\text{Ca}^{2+}]_{\text{free}}$  was calculated using MaxChelator<sup>29</sup>.

### Glucose uptake by PfHT

Uptake of permeant D-[U-<sup>14</sup>C]glucose was measured as described<sup>27</sup>.

### Parasites and parasite culture

Parasites (clones 3D7, HB3 and K1) were cultured and inhibitory constants for drugs assayed as described<sup>2</sup>. The effect of the interaction between two antimalarial agents on the growth of *P. falciparum* in culture was assessed using isobole analysis, as described<sup>30</sup>.

### Confocal microscopy

Cells (at room temperature) were imaged after labelling with BODIPY-thapsigargin (B-7487, Molecular Probes) using a LSM 510 scanning confocal microscope (Carl Zeiss, Jena, Germany), with excitation at 488 nm attenuated to 0.2–0.5% intensity with an acousto-optical tunable filter. Pinhole size was adjusted to give optical sections  $<1.2 \mu\text{m}$ , emission was detected at  $>505 \text{ nm}$  and analysed with LSM 510 software (v.2.01, Carl Zeiss). For imaging of fluorescent artemisinin, medium-term trophozoite-infected

erythrocytes were immobilized using poly-L-lysine coated coverslips in a Biopetechs FCS2 perfusion chamber (maintained at 37 °C in normal growth medium). Fluorescent-labelled artemisinin (500 nM) was added 10 min before imaging.

Received 20 March; accepted 12 May 2003; doi:10.1038/nature01813.

- Hien, T. T. & White, N. J. Qinghaosu. *Lancet* **341**, 603–608 (1993).
- ter Kuile, F., White, N. J., Holloway, P. H., Pasvol, G. & Krishna, S. *Plasmodium falciparum*: In vitro studies of the pharmacodynamic properties of drugs used for the treatment of severe malaria. *Exp. Parasitol.* **76**, 85–95 (1993).
- Jefford, C. W. Why artemisinin and certain synthetic peroxides are potent antimalarials. Implications for the mode of action. *Curr. Med. Chem.* **8**, 1803–1826 (2001).
- Robert, A., Dechy-Cabaret, O., Cazes, J. & Meunier, B. From mechanistic studies on artemisinin derivatives to new modular antimalarial drugs. *Acc. Chem. Res.* **35**, 167–174 (2002).
- Olliaro, P. L., Haynes, R. K., Meunier, B. & Yuthavong, Y. Possible modes of action of the artemisinin-type compounds. *Trends Parasitol.* **17**, 122–126 (2001).
- Meshnick, S. R. Artemisinin: mechanisms of action, resistance and toxicity. *Int. J. Parasitol.* **32**, 1655–1660 (2002).
- Pandey, A. V., Tekwani, B. L., Singh, R. L. & Chauhan, V. S. Artemisinin, an endoperoxide antimalarial, disrupts the hemoglobin catabolism and heme detoxification systems in malarial parasite. *J. Biol. Chem.* **274**, 19383–19388 (1999).
- Haynes, R. K. *et al.* Artemisinin antimalarials do not inhibit hemozoin formation. *Antimicrob. Agents Chemother.* **47**, 1175 (2003).
- O'Neill, P. *et al.* Biomimetic Fe(II)-mediated degradation of artefene (Ro-42-1611). The first EPR spin-trapping evidence for the previously postulated secondary carbon-centered cyclohexyl radical. *J. Org. Chem.* **65**, 1578–1582 (2000).
- Hawley, S. R. *et al.* Relationship between antimalarial drug activity, accumulation, and inhibition of heme polymerization in *Plasmodium falciparum* in vitro. *Antimicrob. Agents Chemother.* **42**, 682–686 (1998).
- Ellis, D. S. *et al.* The chemotherapy of rodent malaria, XXXIX. Ultrastructural changes following treatment with artemisinin of *Plasmodium berghei* infection in mice, with observations of the localization of [<sup>3</sup>H]-dihydroartemisinin in *P. falciparum* in vitro. *Ann. Trop. Med. Parasitol.* **79**, 367–374 (1985).
- Krishna, S. *et al.* Expression and functional characterization of a *Plasmodium falciparum* Ca<sup>2+</sup>-ATPase (PfATP4) belonging to a subclass unique to apicomplexan organisms. *J. Biol. Chem.* **276**, 10782–10787 (2001).
- Toyoshima, C. & Nomura, H. Structural changes in the calcium pump accompanying the dissociation of calcium. *Nature* **418**, 605–611 (2002).
- Price, R. *et al.* The *pfmdr1* gene is associated with a multidrug-resistant phenotype in *Plasmodium falciparum* from the western border of Thailand. *Antimicrob. Agents Chemother.* **43**, 2943–2949 (1999).
- Gu, H. M., Warhurst, D. C. & Peters, W. Uptake of [<sup>3</sup>H] dihydroartemisinin by erythrocytes infected with *Plasmodium falciparum* in vitro. *Trans. R. Soc. Trop. Med. Hyg.* **78**, 265–270 (1984).
- Haynes, R. K. Artemisinin and derivatives: the future for malaria treatment? *Curr. Opin. Infect. Dis.* **14**, 719–726 (2001).
- Meshnick, S. R. *et al.* Iron-dependent free radical generation from the antimalarial agent artemisinin (qinghaosu). *Antimicrob. Agents Chemother.* **37**, 1108–1114 (1993).
- Bray, P. G., Munghin, M., Ridley, R. G. & Ward, S. A. Access to hemozoin: the basis of chloroquine resistance. *Mol. Pharmacol.* **54**, 170–179 (1998).
- Simpson, P. B. & Russell, J. T. Role of sarcoplasmic/endoplasmic-reticulum Ca<sup>2+</sup>-ATPases in mediating Ca<sup>2+</sup> waves and local Ca<sup>2+</sup> release microdomains in cultured glia. *Biochem. J.* **325**, 239–247 (1997).
- Akompong, T., VanWye, J., Ghorri, N. & Haldar, K. Artemisinin and its derivatives are transported by a vacuolar-network of *Plasmodium falciparum* and their anti-malarial activities are additive with toxic sphingolipid analogues that block the network. *Mol. Biochem. Parasitol.* **101**, 71–79 (1999).
- Asawamahsakda, W., Ittarat, I., Pu, Y. M., Ziffer, H. & Meshnick, S. R. Reaction of antimalarial endoperoxides with specific parasite proteins. *Antimicrob. Agents Chemother.* **38**, 1854–1858 (1994).
- Bhisuttibhhan, J. *et al.* The *Plasmodium falciparum* translationally controlled tumor protein homolog and its reaction with the antimalarial drug artemisinin. *J. Biol. Chem.* **273**, 16192–16198 (1998).
- Ono, T. *et al.* Degenerative changes in morphology of *Plasmodium falciparum* induced by artemether in vitro. *Jpn J. Parasitol.* **40**, 587–595 (1991).
- Allen, D. G., Eisner, D. A. & Wray, S. C. Birthday present for digitalis. *Nature* **316**, 674–675 (1985).
- Schatzmann, H.-J. Herzglykoside als Hemmstoffe für den aktiven Kalium- und Natriumtransport durch die Erythrocytenmembran. *Helv. Physiol. Acta* **11**, 346–354 (1953).
- Toyoshima, C., Nakasako, M., Nomura, H. & Ogawa, H. Crystal structure of the calcium pump of sarcoplasmic reticulum at 2.6 Å resolution. *Nature* **405**, 647–655 (2000).
- Woodrow, C. J., Penny, J. I. & Krishna, S. Intraerythrocytic *Plasmodium falciparum* expresses a high-affinity facilitative hexose transporter. *J. Biol. Chem.* **274**, 7272–7277 (1999).
- East, J. M. Purification of a membrane protein (Ca<sup>2+</sup>/Mg<sup>2+</sup>-ATPase) and its reconstitution into lipid vesicles. *Methods Mol. Biol.* **27**, 87–94 (1994).
- Bers, D. M., Patton, C. W. & Nuccitelli, R. A practical guide to the preparation of Ca<sup>2+</sup> buffers. *Methods Cell Biol.* **40**, 3–29 (1994).
- Berenbaum, M. C. A method for testing for synergy with any number of agents. *J. Infect. Dis.* **137**, 122–130 (1978).

**Acknowledgements** We thank T. Joët and A.-C. Uhlemann for discussions, P. Wünnenberg for technical assistance, A. Craig for a *P. falciparum* cDNA library and K. Tanabe for the *P. falciparum* genomic clone 3L6. We thank the charity Hope (Wessex Medical Trust) for financial support of J.M. East, and T. Bolton for access to confocal microscopy. U. E.-L. was funded by the Deutsche Forschungsgemeinschaft, S.A.W. and P.G.B. are funded by the Wellcome Trust and S.K. holds an MRC (UK) grant. This paper is dedicated to the memory of G. Cowan.

**Competing interests statement** The authors declare competing financial interests: details accompany the paper on [www.nature.com/nature](http://www.nature.com/nature).

**Correspondence** and requests for materials should be addressed to S.K. (s.krishna@sghms.ac.uk).

## Feedback regulation of MAPK signalling by an RNA-binding protein

Reiko Sugiura<sup>1</sup>, Ayako Kita<sup>1</sup>, Yasuhito Shimizu<sup>1</sup>, Hisato Shuntoh<sup>2</sup>, Susie O. Sio<sup>1\*</sup> & Takayoshi Kuno<sup>1</sup>

<sup>1</sup>Division of Molecular Pharmacology and Pharmacogenomics, Department of Genome Sciences, Kobe University Graduate School of Medicine, Kobe 650-0017, Japan

<sup>2</sup>Faculty of Health Science, Kobe University School of Medicine, 7-10-2 Tomogaoka, Suma-ku, Kobe 654-0142, Japan

\* Present address: Department of Pharmacology, College of Medicine, University of the Philippines Manila, Manila 1000, Philippines

Mitogen-activated protein kinases (MAPKs) are evolutionarily conserved enzymes that convert extracellular signals into various outputs such as cell growth, differentiation and cell death<sup>1–4</sup>. MAPK phosphatases selectively inactivate MAPKs by dephosphorylating critical phosphothreonine and phosphotyrosine residues<sup>5,6</sup>. The transcriptional induction of MAPK phosphatase expression by various stimuli, including MAPK activation, has been well documented as a negative-feedback mechanism of MAPK signalling<sup>7,8</sup>. Here we show that Rnc1, a novel K-homology-type RNA-binding protein in fission yeast, binds and stabilizes Pmp1 messenger RNA<sup>9</sup>, the MAPK phosphatase for Pmk1 (refs 10, 11). Rnc1 therefore acts as a negative regulator of Pmk1 signalling. Notably, Pmk1 phosphorylates Rnc1, causing enhancement of the RNA-binding activity of Rnc1. Thus, Rnc1 is a component of a new negative-feedback loop that regulates the

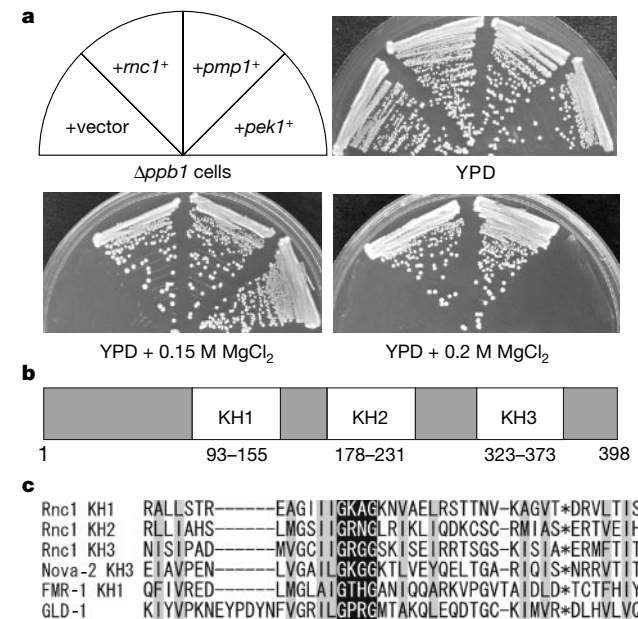


**Figure 1** Identification of Rnc1, a new KH-type RNA-binding protein. **a**, *rnc1*<sup>+</sup> overexpression suppresses the Cl<sup>-</sup> sensitivity of calcineurin deletion ( $\Delta ppb1$ ). Cells were transformed with a multicopy plasmid containing the indicated genes, and streaked onto each plate, then incubated at 30 °C. **b**, Schematic overview of Rnc1. The regions containing the KH motifs are represented by open boxes. Amino acid positions are indicated. **c**, KH-domain sequence alignment in the three KH domains of Rnc1, human Nova-2 KH3, human FMR-1 KH1 and *Caenorhabditis elegans* GLD-1. Black shading denotes the invariant Gly-X-X-Gly segment; grey shading indicates the aliphatic  $\alpha/\beta$  platform; asterisk indicates the variable loop<sup>19</sup>.